Available online at BCREC website: https://bcrec.id

Bulletin of Chemical Reaction Engineering & Catalysis, 18 (3) 2023, 398-406

Research Article

One Pot Synthesis of Calcium Sulfate Hemihydrate from Fishbone-derived Carbon

Teguh Wirawan[1], Mukhamad Nurhadi[2,*], Agung Rahmadani[2], Yuniar Ponco Prananto[3], Zhiying Zhu[4], Sin Yuan Lai[4,5], Hadi Nur[6,7]

[1]*Chemistry Department, Universitas Mulawarman, Kampus Gunung Kelua, Samarinda, 75119, East Kalimantan, Indonesia.*
[2]*Department of Chemical Education, Universitas Mulawarman, Kampus Gunung Kelua, Samarinda, 75119, East Kalimantan, Indonesia.*
[3]*Chemistry Department, Brawijaya University, Malang, 65145, East Java, Indonesia.*
[4]*School of Energy and Chemical Engineering, Xiamen University Malaysia, Selangor Darul Ehsan 43900, Malaysia.*
[5]*College of Chemistry and Chemical Engineering, Xiamen University, Xiamen 361005, China.*
[6]*Department of Chemistry, Universitas Negeri Malang, Malang 65145, Indonesia.*
[7]*Center of Advanced Materials for Renewable Energy (CAMRY), Universitas Negeri Malang, Jl. Semarang No. 5, Malang 65145, Indonesia.*

Received: 19th July 2023; Revised: 3rd September 2023; Accepted: 4th September 2023
Available online: 7th September 2023; Published regularly: October 2023

Abstract

Calcium Sulfate Hemihydrate (CSH) with uniform morphology and high crystallinity were successfully prepared by a precipitation-hydrolysis method in a concentrated sulfuric acid solution containing fishbone-derived carbon. The CSH was produced by carbonization of fishbone powder at 500 °C for 2 h, followed by sulfonation with concentrated sulfuric acid for 3 h. The solid mixture was washed until the pH of 2, then left at room temperature for 3 days. Physical properties of synthesized CSH were characterized using Fourier transform infrared (FTIR) spectroscopy, X-ray diffraction (XRD), wavelength dispersive X-ray fluorescence (WDXRF), Scanning Electron Microscope (SEM), nitrogen adsorption-desorption isotherm, and melting point test. It is concluded that the CSH were formed due to hydrolysis of fishbone-derived carbon in a moderately concentrated sulfuric acid solution of carbon-derived fishbone and crystallization into a fibrous octa calcium phosphate (OCP) form. In this research, effect of crystal growth time, effect of pH during the crystal growth, and effect of volume of the solution were also investigated.

Keywords: Calcium sulfate hemihydrate; carbon; fishbone; carbonization; sulfonation

How to Cite: T. Wirawan, M. Nurhadi, A. Rahmadani, Y.P. Prananto, Z. Zhu, S.Y. Lai, H. Nur (2023). One Pot Synthesis of Calcium Sulfate Hemihydrate from Fishbone-derived Carbon. *Bulletin of Chemical Reaction Engineering & Catalysis*, 18(3), 398-406 (doi: 10.9767/bcrec.19515)

Permalink/DOI: https://doi.org/10.9767/bcrec.19515

1. Introduction

Calcium sulfate hemihydrate ($CaSO_4.0.5H_2O$, or CSH) is a kind of sub-nanoscale mineral, and its morphology is oriented by the differential growth velocity between axial and lateral directions. CSH or bassanite or plaster of Paris has been extensively used in buildings, ceramics and medical industries [1]. CSH is potential reinforce materials which used in a wide range of applications such as rubber, plastics, antifriction materials, and paper [2].

* Corresponding Author.
Email: nurhadi1969@yahoo.co.id (M. Nurhadi)

CSH has become popular due to its special properties, such as high aspect ratio [3,4], high tensile strength and elastic modulus [5], ease of surface modification [6], ease of dispersion [7], integrated internal structure [8], and nontoxicity [9].

In recent years, new technologies for preparing CSH have been extensively developed. Wang *et al*. [10] prepared CSH using sulfuric acid (H_2SO_4) was added dropwise to a $Ca(OH)_2$, the powder was added to calcium chloride ($CaCl_2$). Fukugaichi and Matsue [11] obtained CSH by using solid calcite ($CaCO_3$) as a starting material and mixing it with dilute sulfuric acid (H_2SO_4) in methanolic solution. Fu *et al*. [12] prepared CSH by using $CaCl_2$ solution mixed with calcium sulfate dihydrate ($CaSO_4.2H_2O$) in the reactor, the powder obtained by vacuum filtration was quickly rinsed with boiling water to remove residual $CaCl_2$, and then with isopropanol to remove water. Xu *et al*. [13] obtained CSH using the desulfurization of gypsum that composed mainly of $CaSO_4.2H_2O$ and $CaCO_3$ and then treated with dilute H_2SO_4 at room temperature to convert $CaCO_3$ to $CaSO_4$; the latter was then heated at 110–150 °C to form CSH. Wang *et al*. [14,15] prepared CSH using purified flue-gas desulfurization (FGD) gypsum as the raw material by hydrothermal crystallization in H_2SO_4-H_2O solution, and the diameters of the CSH ranged from 1 to 3 μm, and the average aspect ratio was higher than 200. Jiang *et al*. [16] synthesized CSH by a two-step method, in which the precursor was prepared in the first step, and the CSH was produced in the second step. Most studies have focused on technological modification or the mechanism of the preferred orientation growth that used pure grade chemicals as the raw materials, thus it is costly. However, little effort has been explored for wastes, like fishbone as raw materials to produce CSH.

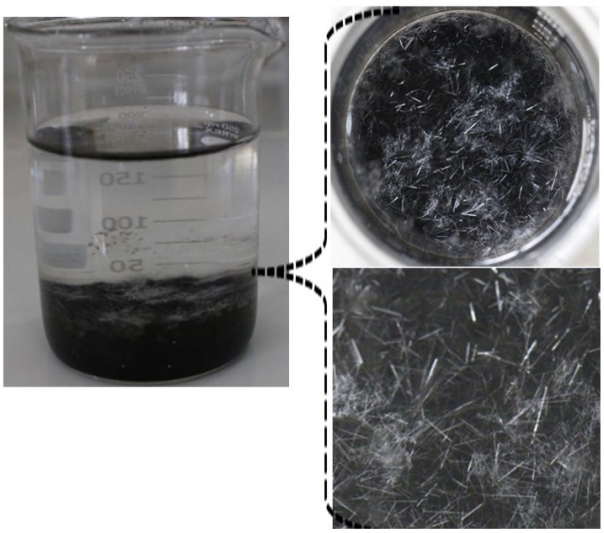

Figure 1. Formation of Calcium Sulfate Hemihydrate (CSH).

In our study, calcium sulfate hemihydrate or bassanite (CSH; $CaSO_4.0.5H_2O$) have been successfully synthesized in one-pot reaction at room temperature using fishbone as a starting material. Firstly, the powder of fishbone was carbonized and then the fishbone-derived carbon was mixed with concentrated sulfuric acid under stirring for 3 h. Then it was washed by using distillate water until the pH of 2, and left at room temperature for 3 days until CSH grown to be harvested. This synthesis technique decomposes organic components in bones via carbonization process, subsequently the CSH can be formed via sulfonation process. In this research, we also investigated the effect of time duration, the effect of pH and the effect of volume of solution. The CSH were characterized by WDXRF, FTIR, XRD, SEM, nitrogen adsorption-desorption isotherm, and melting point test.

2. Materials and Methods

2.1 Carbonization Process

The fish bone was collected from many food companies around Samarinda, East Kalimantan, Indonesia. The fish bones were separated from other impurities by washing with boiling water. The fish bone was dried on oven at 110 °C for overnight. The fish bone powder was obtained by crushing, then the powder was carbonized in a furnace at 500 °C for 2 h to form carbon. The fish bone-derived carbon (FBC) at desired temperature (T) is labeled as FBCT. For example, FBC500 is the fish bone-derived carbon prepared via carbonization at 500 °C for 2 h.

2.2 Crystallization Process

Every gram the FBC500 was immersed in 6 mL of concentrated sulfuric acid (H_2SO_4; JT Beker). The mixture was stirred at room temperature for 3 h and washed with distillate water to remove any loosely bound acid until pH of filtrate 2. The FBC500 solution was saved at room temperature for three days until the crystal growth (Figure 1). Then, decantation and filtration were conducted to separate carbon and crystal. The crystal was washed until the filtrate reached neutral pH. The crystal then dried at 110 °C for overnight. In this research, the effect of pH (1, 2, 3, and 4), solution volume

(100, 300 and 600 mL), and reaction duration (1, 3, and 6 day) were studied.

2.4 Crystals Characterizations

The crystal was characterized by WDXRF, FTIR, XRD, SEM, nitrogen adsorption-desorption isotherm, and melting point test. The chemical composition from the crystal was investigated by using 1 kW wavelength dispersive X-ray fluorescence (WDXRF PANalytical, Minipal 4). Functional group in the crystal were identified using FTIR spectrometer (IR−Prestige−21 Shimadzu) with a spectral resolution of 2 cm^{-1}, scans of 10 s, at 20 °C and range of wavenumber from 400 to 4000 cm^{-1}. The XRD instrument (Phillips PANalytical X'Pert PRO) was used to determine the crystallinity and phase content of the crystal with the Cu-K_α (λ = 1.5406 Å) radiation as the diffracted monochromatic beam at 40 kV and 40 mA and the pattern was scanned in the 2θ ranges between 7° and 60° at a step 0.03° and step time 1 s. The surface morphology of crystal was determined by using the SEM (FEI Inspect S50) instrument with an accelerating voltage of 15 kV. A brief thermal analysis of the crystal was done by melting point test using open capillary tube. The surface area, pore-volume, and pore size distribution were determined by nitrogen adsorption-desorption isotherms that were created from the data collected from a Quantachrome Nova 1200e instrument.

3. Results and Discussion

The wavelength dispersive X-ray fluorescence (WDXRF) is used to determine the chemical compositions of inorganic compounds [17–20]. WDXRF results show that the fish bone-derived carbon 500 (FBC500) contains calcium (Ca), magnesium (Mg), phosphorus (P), and potassium (K) [17]. The fish bone-derived carbon consists of valuable elements which can be used as biomedical product, like calcium sulfate hemihydrate (CSH). The CSH consists of major elements, such as calcium (Ca), sulfur (S), samarium (Sm), and molybdenum (Mo). The inorganic phase of these samples is composed of minor constituents, including magnesium (Mg), phosphorus (P), vanadium (V), and germanium (Ge). The complete list of elements and compounds is presented in Table 1. Moreover, based on WDXRF results and calculation, the Ca/P ratio of the crystal was 128.5, which indicate that this high Ca/P ratio may lead to the transformation of crystal structure to other phase (tri-calcium phosphate) [21,22].

Table 1. Elements analysis of FBC500 and CSH obtained using WDXRF.

Element (wt%)	FBC500	CSH
Mg	0.4	0.10
P	16.8	0.34
S	-	23.00
K	0.02	-
Ca	49.5	43.70
Cr	0.23	-
V	-	0.21
In	1.1	-
La	0.8	-
Ge	-	1.00
Mo	-	9.70
Sm	31	21.00

FTIR spectra of (a) FBC500 and (b) CSH are shown in Figure 2. The spectra of FBC(500) show absorption bands around 2500−3600 cm^{-1} are corresponded to the stretching of hydroxyl (O−H) group of organic compounds in the FBC500. The presence of carbonate ion (CO_3^{2-}) and phosphate ion (PO_4^{3-}) groups could prove that the presence of hydroxyapatite (HA) in the sample [23–28]. The carbonate ion (CO_3^{2-}) was confirmed by the bands at 1272 and 1108 cm^{-1} which correlated with the C−O stretching. The phosphate ion (PO_4^{3-}) groups, which correlated with the P−O stretching asymmetric absorption bands around 1150–1000 cm^{-1}, is known as the characteristics of bands for HA. The bending vibration of PO_4^{3-} was observed by bands located at 510–620 cm^{-1}. The bands at 874 cm^{-1}, was assigned to the acidic phosphate group (HPO_4^{2-}) [29]. FTIR spectra of CSH show the absorption band at 3613, 3559, and 1626

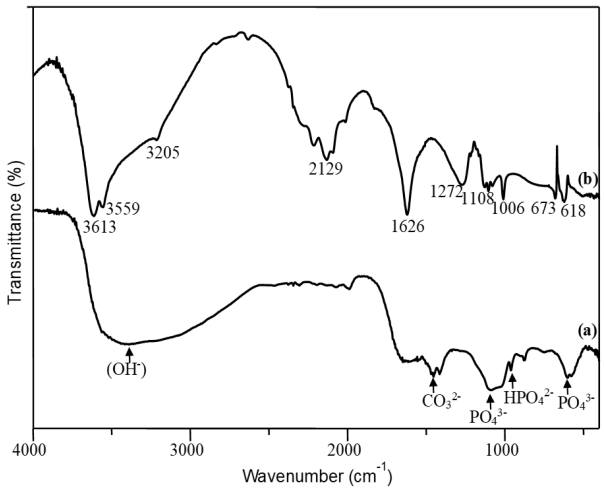

Figure 2. FTIR spectra of (a) FBC500 and (b) CSH.

cm^{-1} associated with crystal water molecule combined on ($CaSO_4$) [30–32]. The characteristic bands of $CaSO_4$ can be investigated by the bands at 1272 cm^{-1} can be assigned to Ca^{2+} and the band at 1108, 1006, 673, and 618 cm^{-1} can be assigned to SO_4^{2-} stretching. [33].

Powder diffraction pattern and crystallinity of (a) FBC500 and (b) CSH were shown in Figure 3. In Figure 3(a), the HA crystallinity (JCPDS-PDF 74-0565) of FBC500 was shown by the diffraction peaks at 2θ angles of 25.8, 32.0, 39.7, 46.8, 49.4, and 53°. The diffraction peaks in Figure 2(a) are probably due to there is carbon impurity that mixed with HA crystal. The XRD pattern (Figure 3(b)) verified the formation of CSH (JCPDS card No. 14-0453) can be assigned by the characteristic peaks at 2θ angles of 14.7, 25.7, 29.8, 31.9, and 49.4°

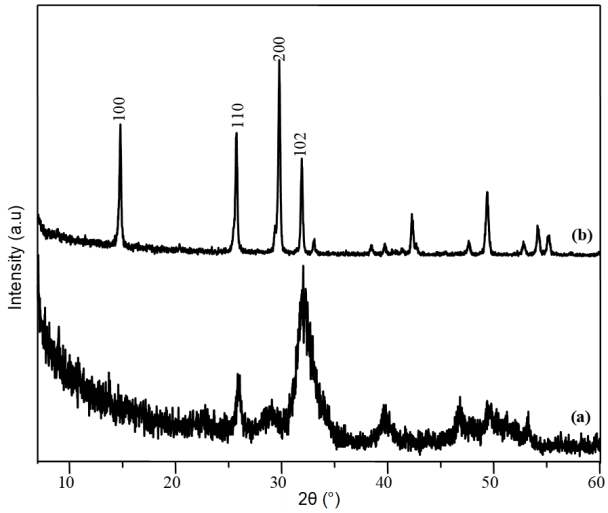

Figure 3. XRD pattern of (a) FBC500 and (b) CSH.

and are parallel to the preferred direction of growth [34,35]. Average crystallite size (T) of CSH (Figure 3(b)) is also calculated, which is based on Debye-Scherrer's equation [36]:

$$T = \frac{K\lambda}{\beta \cos\theta} \quad (1)$$

where, T is the average of crystal size, K = constant dependent on crystallite shape, $0.8 < K < 1.1$; K = 0.94 for FWHM of spherical crystals with cubic symmetry; λ is the wavelength of monochromatic radiation (0.15406 nm), β is defined as the full width of peak from the intensity distribution pattern measured at half of the maximum intensity value (FWHM = 0.189; 0.189; 0.199; 0.278; 0.219) on the range 2θ = 20 to 60 scale in radians and θ is the Bragg angle of the peak in degrees. The average crystal size of CSH was estimated to be 41.87 nm, which suggest that the CSH - derived the carbon from fish bone was nanocrystalline in nature.

SEM images of (a) FBC500 (magnification of 5000×), (b) CSH (magnification of 100×), and (c) CSH (magnification of 5000×) are displayed in Figure 4. In Figure 4(a), an overview of FBC500 particles appear in clumps with irregular shape [28]. Under the same magnification as Figure 4(a), Figure 4(c) CSH particles exhibits in cuboid shape. To zoom out under magnification of 100× for an overview, Figure 4(b) depicts that the CSH particles in the form of a long block needle-shaped single crystal with a flat-cracked surface. CSH is the α-hemihydrate comprises well-formed transparent idiomorphic crystals with sharp crystal edges. The morphology of the CSH synthesized from fishbone-derived carbon was in line with that or reported from previous work [38,39].

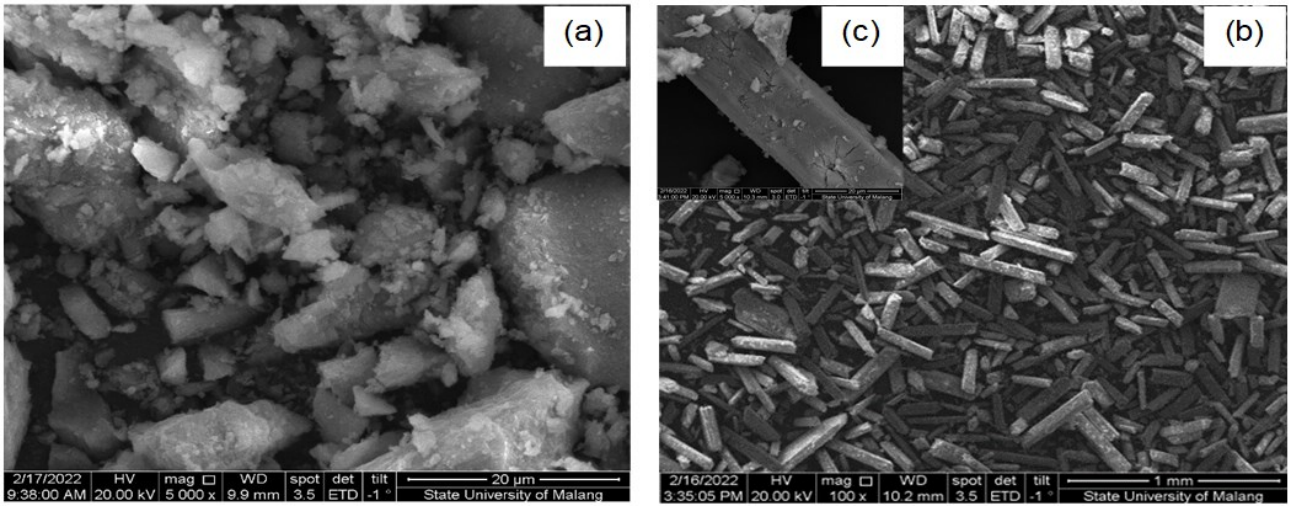

Figure 4. SEM Image of (a) FBC500 (magnification of 5000×), (b) CSH (magnification of 100×), and (c) CSH (magnification of 5000×).

Based on Figure 5, thermal analyses of the crystal by DTA-TGA reveal that the crystals undergo one-stage decomposition from around 110 °C to 160 °C. At this temperature, about 40% reduction is observed, which is predicted due to the loss of water molecules, resulting in the anhydrate form of the sample. This anhydrate compound remains stable up to 500 °C.

Mechanism for CSH formation is proposed in this study: H_2SO_4 solution was used to dissolve the calcium embedded in the carbon from fish bone. The CSH molecules are dissolved and released from the carbon from fish bone. The presence of H^+ ions supplied from H_2SO_4 will prohibit the fast aggregation of CSH molecules. The fast aggregation will cause agglomeration and amorphous phase tend to be formed. With the appropriate concentration of H^+, CSH will re-organize themselves into crystal seeds, followed by nucleation, which eventually it started to grow slowly into bigger crystalline CSH.

Surface area, pore volume, and pore size of FBC500 and CSH were analyzed with nitrogen adsorption-desorption isotherm mechanism. The surface area, pore volume and mean pore size are presented in Table 2. The mean pore size of both samples are more than 2 nm and less than 50 nm, which indicate a uniform mesopores were yielded. The evident of mesopores in FBC500 and CSH can be seen from knee area in the physisorption isotherms (Figure 6).

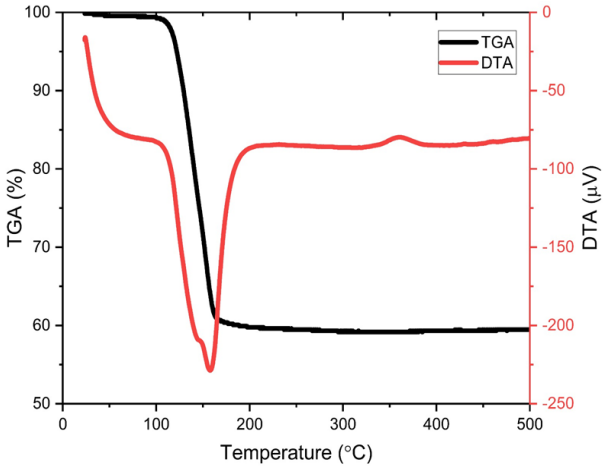

Figure 5. TGA and DTA curves of CSH.

3.1 The Effect of pH

The effect of pH on CSH crystal growth can be observed from the XRD pattern in Figure 7. The CSH crystal grew well at pH 1 and 2 after the sulfonation process, which shown by the characteristic peaks at 2θ angles of 14.7, 25.7, 29.8, 31.9, and 49.4° which correspond to the CSH crystal. In Figure 7 (a and b), the characteristic peaks at 2θ angles of 14.7, 25.7, 29.8, 31.9, and 49.4° were absence, which indicates that the CSH crystal does not yielded in pH 3 and 4 after the sulfonation process.

3.2 The Effect of Solution Volume

The effect of the total volume of the solution with pH 2 on CSH crystal growth can be studied based on the XRD pattern in Figure 8. The total volume of solution after the sulfonation

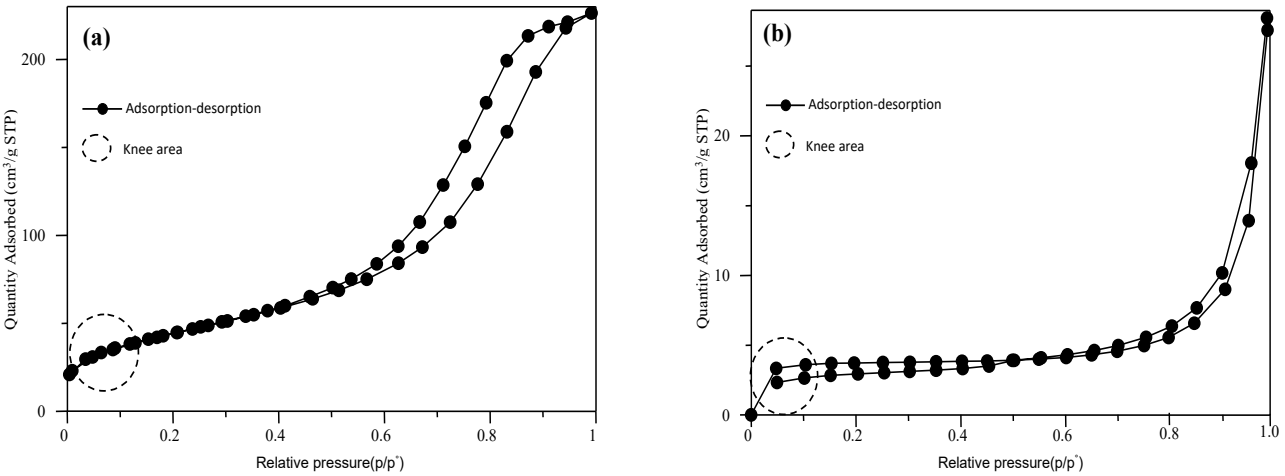

Figure 6. The physisorption isotherms of (a) FBC500 and (b) CSH.

Table 2. Physical properties of the samples.

Samples	BET surface area (m^2/g)	Pore Volume (cm^3/g)	Mean pore size (nm)
FBC500	90.8	0.237	5.2
CSH	11.3	0.043	7.5

process at pH 2 is related to the amount of sulfate ions (SO_4^{2-}) as the main component of calcium sulfate hemihydrate. In Figure 8(a), a total volume of 100 mL is insufficient to support the CSH crystal growth, which is shown by the absence of the characteristic peaks at 2θ angles of 14.7, 25.7, 29.8, 31.9, and 49.4°. On the other hand, total volumes of solution of 300 and 600 mL (Figure 8(b and c)) is sufficient to support the growth of CSH crystal, which is supported by the presence of the characteristic peaks at 2θ angles of 14.7, 25.7, 29.8, 31.9, and 49.4° appear. Hence, it can be concluded the more volume used, the higher the number of sulfate ions presence, which eventually lead to higher possibility of CSH to be crystallized.

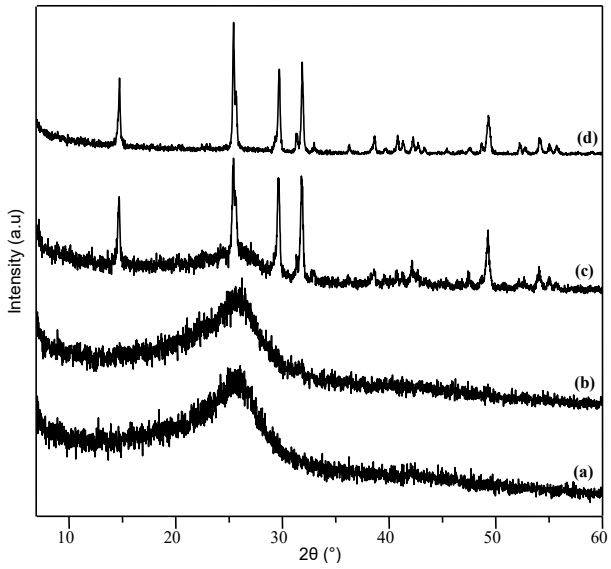

Figure 7. XRD pattern of CSH due to the effect of pH for (a) 4, (b) 3, (c) 2 and (d) 1.

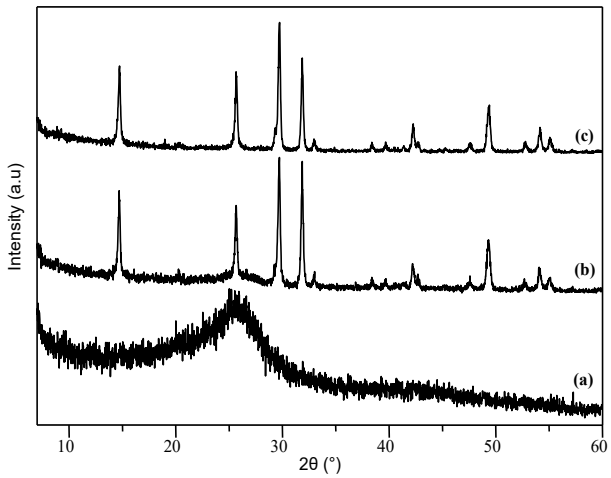

Figure 8 XRD pattern of CSH due to the effect of volume solution for (a) 100 mL (b) 300 mL and (b) 600 mL.

3.3 The Effect of Duration Time of Crystal Growth

The effect of the time of the CSH crystal growth can be observed from the XRD pattern in Figure 9. In Figure 9(a), the characteristic peaks at 2θ angles of 14.7, 25.7, 29.8, 31.9, and 49.4° that indicate the CSH crystal were absence when the solution was stand only for 1 day. After three days of crystal growth, the CSH crystals were observed.

4. Conclusions

In this study, colorless calcium sulfate hemihydrate (CSH) was successfully obtained by one pot reaction. The CSH crystal was fabricated from fishbone by carbonization and sulfonation process. The organic components in fishbones were decomposed via carbonization process and the CSH was formed via sulfonation process. The WDXRF analysis reveals that a higher Ca/P ratio prompts a transformation in crystal structure, transitioning it into tricalcium phosphate. The FTIR spectra of FBC500 corroborate the presence of HA in the sample. A comparison between the FTIR spectra of FBC500 and CSH highlights a noteworthy distinction: CSH exhibits an absorption band corresponding to crystal water, whereas FBC500 solely displays an absorption band for hydroxyl groups. This divergence suggests that FBC500 contains a higher concentration of organic compounds compared to CSH. FBC500's crystallinity wasn't distinct because carbon impurity mixed with HA crystal, whereas CSH was subjected to testing that yielded high crystallinity results. From the SEM images, it becomes evident that FBC500 particles assume an irregular shape, contrasting with the well-

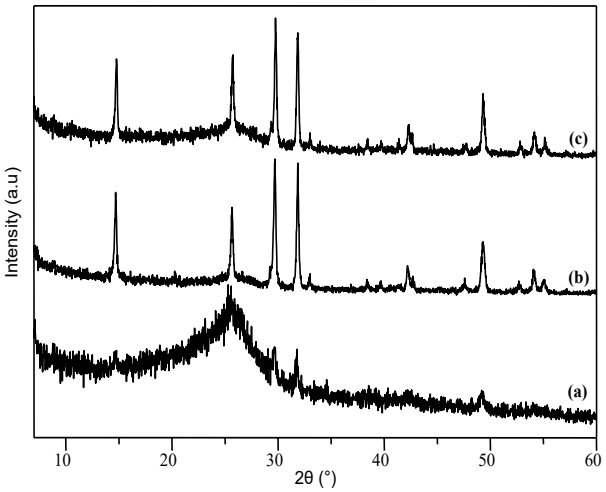

Figure 9. XRD pattern of CSH due to the effect of time for (a) 1 day (b) 3 day and (c) 6 day.

defined form of CSH particles – characterized by elongated, block needle-shaped single crystals and a flat-cracked surface. Thermal analysis proves that CSH can stable up to 500 °C. Following the sulfonation process, CSH crystals exhibit robust growth at pH levels of 1 and 2. Notably, a total solution volume of 300 and 600 mL respectively fosters the growth of CSH crystals effectively. However, it is important to note that the observation of CSH crystals requires a span of three days for their growth to manifest.

Acknowledgements

Authors gratefully acknowledge The *Direktorat Jenderal Pendidikan Tinggi, Riset, dan Teknologi, Kementerian Pendidikan, Kebudayaan, Riset, dan Teknologi, Republik Indonesia Tahun Anggaran* 2023 (contract number: 502/UN17.L1/HK/2023).

CRedit Author Statement

Author Contributions: T. Wirawan: Conceptualization, Methodology, Investigation, Resources, Data Curation, Writing, Writting Draft Preparation. M. Nurhadi: Conceptualization, Methodology, Investigation, Resources, Data Curation, Writing, Review and Editing, Supervision; A. Rahmadani: Conceptualization, Methodology, Formal Analysis, Data Curation, Writting Draft Preparation, Project Administration; Y. P. Prananto: Validation, Writing, Review and Editing, Data Curation; Zhiying Zhu: Writing, Review and Editing; S. Y. Lai : Proofreading, Writing, Review and Editing.; H. Nur: Proofreading, Writing, Review and Editing. All authors have read and agreed to the published version of the manuscript.

References

[1] Singh, N.B., Middendorf, B. (2007). Calcium sulphate hemihydrate hydration leading to gypsum crystallization. *Progress in Crystal Growth and Characterization of Materials,* 53, 57-77. DOI: 10.1016/j.pcrysgrow.2007.01.002

[2] Xin, Y., Hou, S.C., Xiang, L., Yu, Y.-X. (2015). Adsorption and substitution effects of Mg on the growth of calcium sulfate hemihydrate: An ab initio DFT study. *Applied Surface Science,* 357, 1551-1557. DOI: 10.1016/j.apsusc.2015.09.223

[3] Hou, S.C., Xiang, L. (2013). Influence of activity of $CaSO_4 \cdot 2H_2O$ on hydrothermal formation of $CaSO_4 \cdot 0.5H_2O$ whiskers. *Journal of Nanomaterials,* 2013, 2-7. DOI: 10.1155/2013/237828

[4] Zhao, W., Wu, Y., Xu, J., Gao, C. (2015). Effect of ethylene glycol on hydrothermal formation of calcium sulfate hemihydrate whiskers with high aspect ratios. *RSC Advances,* 5(62), 50544–50548. DOI: 10.1039/c5ra07712e

[5] Chen, S., Wang, Q., Wang, T. (2011). Mechanical, damping, and thermal properties of calcium sulfate whisker-filled castor oil-based polyurethane/epoxy ipn composites. *Journal of Reinforced Plastics and Composites,* 30(6), 509-515. DOI: 10.1177/0731684411398539

[6] Wang, J., Yang, K., Lu, S. (2015). Preparation and characteristic of novel silicone rubber composites based on organophilic calcium sulfate whisker. *High Performance Polymers,* 23(2), 141-150. DOI: 10.1177/0954008310395415

[7] Yuan, W., Cui, J., Cai, Y., Xu, S. (2015). A novel surface modification for calcium sulfate whisker used for reinforcement of poly(vinyl chloride), *Journal of Polymer Research,* 22(173), 1-9. DOI 10.1007/s10965-015-0813-4

[8] Han, Q., Luo, K., Li, H., Xiang, L. (2014). Influence of disodium hydrogen phosphate dodecahydrate on hydrothermal formation of hemihydrate calcium sulfate whiskers. *Particuology,* 17, 131-135. DOI: 10.1016/j.partic.2013.10.002

[9] Xu, A.-Y., Li, H.-P., Luo, K.-B., Xiang, L. (2011). Formation of calcium sulfate whiskers from $CaCO_3$-bearing desulfurization gypsum. *Research on Chemical Intermediates,* 37, 449-455. DOI: 10.1007/s11164-011-0283-1

[10] Wang, P., Lee, E.-J., Park, C.-S., Yoon, B.-H., Shin, D.-S., Kim, H.-E. (2008). Calcium Sulfate Hemihydrate Powders with a Controlled Morphology for Use as Bone Cement. *Journal of the American Ceramic Society,* 91(6), 2039-2042. DOI: 10.1111/j.1551-2916.2008.02358.x

[11] Fukugaichi, S., Matsue, N. (2018). One-Step Synthesis of Calcium Sulfate Hemihydrate Nanofibers from Calcite at Room Temperature. *ACS Omega,* 3(3), 2820-2824. DOI: 10.1021/acsomega.7b01994

[12] Fu, L., Xia, W., Mellgren, T., Moge, M., Engqvist, H. (2017). Preparation of High Percentage α-Calcium Sulfate Hemihydrate via a Hydrothermal Method, *Journal of Biomaterials and Nanobiotechnology,* 8, 36-49. DOI: 10.4236/jbnb.2017.81003

[13] Xu, A.-Y., Li, H.-P., Luo, K.-B., Xiang, L. (2011). Formation of calcium sulfate whiskers from $CaCO_3$-bearing desulfurization gypsum, *Research on Chemical Intermediates,* 37(2), 449-455. DOI: 10.1007/s11164-011-0283-1

[14] Wang, X., Yang, L., Zhu, X., Yang, J. (2014). Preparation of calcium sulfate whiskers from FGD gypsum via hydrothermal crystallization in the H_2SO_4–NaCl–H_2O system. *Particuology*, 12, 42-48. DOI: 10.1016/j.partic.2013.12.001

[15] Liu, C., Zhao, Q., Wang, Y., Shi, P., Jiang, M. (2016). Hydrothermal synthesis of calcium sulfate whisker from flue gas desulfurization gypsum. *Chinese Journal of Chemical Engineering,* 24(11), 1552-1560. DOI: 10.1016/j.cjche.2016.04.024

[16] Jiang, N., Zhang, C., Xue, C., Dang, L., Xu, S. (2018). In situ synthesis of hydrophobic calcium sulfate hemihydrate whiskers. *Materials Research Express,* 5, 1-7. DOI: 10.1088/2053-1591/aace63

[17] Lestari, S., Nurhadi, M., Kusumawardani, R., Saputro, E., Pujisupiati, R., Muskita, N.S., Fortun, N., Purwandari, A.S.,Aryani, F., Lai, S.Y., Nur, H. (2022). Comparative Adsorption Performance of Carbon-containing Hydroxyapatite Derived Tenggiri (Scomberomorini) and Belida (Chitala) Fish Bone for Methylene Blue. *Bulletin of Chemical Reaction Engineering & Catalysis,* 17(3), 565-576. DOI: 10.9767/bcrec.17.3.15303.565-576

[18] Raynaud, S., Champion, E., Bernache-Assollant, D., Laval, J.-P. (2001). Determination of Calcium/Phosphorus Atomic Ratio of Calcium Phosphate Apatites Using X-Ray Diffractometry. *Journal of the American Ceramic Society,* 84(2), 59-66. DOI: 10.1111/j.1151-2916.2001.tb00663.x

[19] Babos, D.V., Costa, V.C., Sperança, M.A., Pereira-Filho, E.R. (2018). Direct determination of calcium and phosphorus in mineral supplements for cattle by wavelength dispersive X-ray fluorescence (WD-XRF). *Microchemical Journal,* 137, 272-276. DOI: 10.1016/j.microc.2017.11.002

[20] Costa, V.C., Amorim, F.A.C., Babos, D.V.d., Pereira-Filho, E.R. (2019). Direct determination of Ca, K, Mg, Na, P, S, Fe and Zn in bivalve mollusks by wavelength dispersive X-ray fluorescence (WDXRF) and laser-induced breakdown spectroscopy (LIBS). *Food Chemistry,* 273, 91-98. DOI: 10.1016/j.foodchem.2018.02.016

[21] Lu, B.-Q., Willhammar, T., Sun, B.-B., Hedin, N., Gale, J.D., Gebauer, D. (2020). Introducing the crystalline phase of dicalcium phosphate monohydrate. *Nature Communications,* 11, 1-8. DOI: 10.1038/s41467-020-15333-6

[22] Hoeher, A.J., Mergelsberg, S.T., Borkiewicz, O.J., Michel, F.M. (2021). Impacts of Initial Ca/P on Amorphous Calcium Phosphate. *Crystal Growth & Design,* 21(7), 3736-3745. DOI: 10.1021/acs.cgd.1c00058

[23] Chakraborty, R., RoyChowdhury, D. (2013). Fish bone derived natural hydroxyapatite-supported copper acid catalyst: Taguchi optimization of semibatch oleic acid esterification. *Chemical Engineering Journal,* 215–216, 491–499. DOI: 10.1016/j.cej.2012.11.064

[24] Patel, S., Han, J., Qiu, W., Gao, W. (2015). Synthesis and characterisation of mesoporous bone char obtained by pyrolysis of animal bones, for environmental application. *Journal of Environmental Chemical Engineering,* 3, 2368-2377. DOI: 10.1016/j.jece.2015.07.031

[25] Yin, T., Park, J. W., Xiong, S. (2015). Physicochemical properties of nano fish bone prepared by wet media milling. *LWT - Food Science and Technology,* 64(1), 367-373. DOI: 10.1016/j.lwt.2015.06.007

[26] Zayed, E.M., Sokker, H.H., Albishri, H.M., Farag, A.M. (2013). Potential use of novel modified fishbone for anchoring hazardous metal ions from their solutions. *Ecological Engineering,* 61, 390–393. DOI: 10.1016/j.ecoleng.2013.09.010

[27] Szpak, P. (2011). Fish bone chemistry and ultrastructure: implications for taphonomy and stable isotope analysis. *Journal of Archaeological Science,* 38(12), 3358-3372. DOI: 10.1016/j.jas.2011.07.022

[28] Boutinguiza, M., Poua, J., Comesaña, R., Lusquiños, F., Carlos, A.d., Leóna, B. (2012). Biological hydroxyapatite obtained from fish bones. *Materials Science and Engineering: C,* 32(3), 478-486. DOI: 10.1016/j.msec.2011.11.021

[29] Jaber, H.L., Hammood, A.S., Parvin, N. (2017). Synthesis and characterization of hydroxyapatite powder from natural Camelus bone, *Journal of the Australian Ceramic Society,* 54(1), 1-10. DOI: 10.1007/s41779-017-0120-0

[30] Liu, C., Zhao, Q., Wang, Y., Shi, P., Jiang, M. (2016). Surface modification of calcium sulfate whisker prepared from flue gas desulfurization gypsum. *Applied Surface Science.,* 360, 263-269. DOI: 10.1016/j.apsusc.2015.11.032

[31] Feng, X., Zhang, Y., Wang, G., Miao, M., Shi, L. (2015). Dual-surface modification of calcium sulfate whisker with sodium hexametaphosphate/silica and use as new water-resistant reinforcing fillers in papermaking. *Powder Technology,* 271, 1-6. DOI: 10.1016/j.powtec.2014.11.015

[32] Dang, L., Nai, X., Zhu, D., Jing, Y., Liu, X., Dong, Y., Li, W. (2014). Study on the mechanism of surface modification of magnesium oxysulfate whisker. *Applied Surface Science,* 317, 325-331. DOI: 10.1016/j.apsusc.2014.07.205

[33] Jiang, N., Zhang, C., Xue, C., Dang, L., Xu, S. (2018). In situ synthesis of hydrophobic calcium sulfate hemihydrate whiskers. *Materials Research Express,* 5, 1-7. DOI: 10.1088/2053-1591/aace63

[34] Qi, Y., Zeng, C., Wang, C., Ke, X., Zhang, L. (2017). Continuous fabrication of calcium sulfate whiskers with adjustable aspect ratio in microdroplets. *Materials Letters,* 194, 231-233. DOI: 10.1016/j.matlet.2017.02.066

[35] Mao, X., Song, X., Lu, G., Sun, Y., Xu, Y., Yu, J. (2014). Effects of Metal Ions on Crystal Morphology and Size of Calcium Sulfate Whiskers in Aqueous HCl Solutions. *Industrial & Engineering Chemistry Research,* 53(45), 17625–17635. DOI: 10.1021/ie5030134

[36] Kusumawardani, R., Nurhadi, M., Wirhanuddin, W., Gunawan, R., Nur, H. (2019). Carbon-containing Hydroxyapatite Obtained from Fish Bone as Low-cost Mesoporous Material for Methylene Blue Adsorption. *Bulletin of Chemical Reaction Engineering & Catalysis,* 14(3), 660-671. DOI: 10.9767/bcrec.14.3.5365.660-671

[37] Abdullah, N.H., Noor, A.M., Mat Rasat, M.S., Mamat, S., Mohamed, M., Mohd Shohaimi, N.A., Mohd Amin, M.F. (2020). Preparation and Characterization of Calcium Hydroxyphosphate (Hydroxyapatite) from Tilapia Fish Bones and Scales via Calcination Method. *Materials Science Forum,* 1010, 596-601. DOI:10.4028/www.scientific.net/MSF.1010.596

[38] Wang, P., Lee, E.-J., Park, C.-S., Yoon, B.-H., Shin, D.-S., Kim, H.-E. (2008). Calcium Sulfate Hemihydrate Powders with a Controlled Morphology for Use as Bone Cement. *Journal of the American Ceramic Society,* 91(6), 2039-2042. DOI: 10.1111/j.1551-2916.2008.02358.x

[39] Liu, C., Zhao, Q., Wang, Y., Shi, P., Jiang, M. (2016). Hydrothermal synthesis of calcium sulfate whisker from flue gas desulfurization gypsum. *Chinese Journal of Chemical Engineering,* 24(11), 1552-1560. DOI: 10.1016/j.cjche.2016.04.024